THE SPECTRUM OF SMALL PERTURBATIONS IN PLANE COUETTE-POISEUILLE FLOW

A. M. Sagalakov

The spectrum of small perturbations of plane Couette-Poiseuille flow is studied. The perturbations are classified according to their behavior at large wave numbers. The changes in the spectrum are traced as the transition is made from Poiseuille to Couette flow at fixed Reynolds number. The behavior of the perturbations is considered as a function of the Reynolds number.

1. We consider the stationary flow of a viscous incompressible fluid between parallel plates due to a pressure gradient and the relative motion of the plates. The problem of hydrodynamical stability can be reduced to the analysis of the spectrum of the eigenvalues of the Orr-Sommerfeld equation

$$\varphi^{IV} - 2\alpha^2\varphi^{II} + \alpha^4\varphi = i\alpha R\,[(u-c)(\varphi^{II} - \alpha^2\varphi) - u''\varphi] \tag{1.1}$$

with boundary conditions

$$\varphi(\pm 1) = \varphi'(\pm 1) = 0 \tag{1.2}$$

Here $\varphi(y)$ is the amplitude of the perturbation stream function, α is the wave number, R is the Reynolds number, u is the velocity profile, and $c = X + iY$ is the complex phase velocity of the perturbation, the eigenvalue of the problem. Negative values of Y correspond to damping of the perturbation, and positive values to increase in the perturbations. As the unit of length we take the half-width of the channel, and as the unit of velocity we take the sum of the stream velocity on the axis and the velocity of the upper plate at $y = 1$. The expression for u has the form

$$u = (1 - A)(1 - y^2) + Ay \tag{1.3}$$

In studying the eigenvalue problem (1.1), (1.2) most frequently the discussion is restricted to neutral perturbations. But in a number of problems, for example, in the development of nonlinear theory, we have to study the whole spectrum of small perturbations.

The whole spectrum of small perturbations has not previously been studied for asymmetric profiles. Neutral perturbations in the type of flow under consideration were studied by Potter [1] and Hains [2], who obtained results which agreed well.

2. For given A, R, α there is a countable number of eigenvalues c_n. For large and small α we can obtain asymptotic expressions for the c_n. If we use the results obtained in [3] it is easy to find asymptotic expressions for the eigenvalues for small α. They have the form

$$Y_n = -\delta_n(\alpha R)^{-1} \tag{2.1}$$

Novosibirsk. Translated from Zhurnal Prikladnoi Mekhaniki i Tekhnicheskoi Fiziki, No. 2, pp. 63-67, March-April, 1971. Original article submitted November 20, 1969.

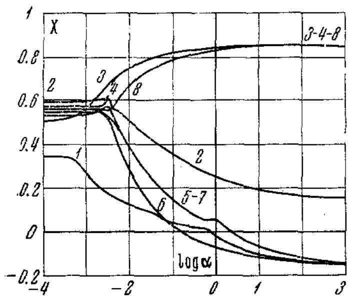

Fig. 1

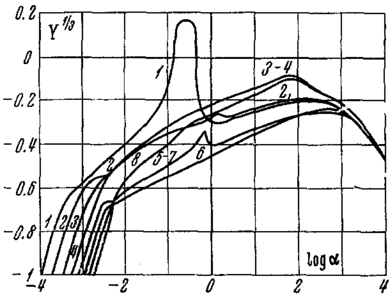

Fig. 2

$$X_n = (1 - A)\left[{}^2/_3 - 5(2\delta_n)^{-1}\right] \qquad (n = 1, 3, 5, \ldots)$$
$$X_n = (1 - A)\left[{}^2/_3 + 5(6\delta_n)^{-1}\right] \qquad (n = 2, 4, 6, \ldots) \qquad (2.2)$$
$$\delta_n = {}^1/_4\pi^2(n+1)^2 \qquad (n = 1, 3, 5, \ldots)$$

For $n = 2, 4, 6, \ldots$, the value of δ_n is found from the equation

$$\operatorname{tg}\sqrt{\delta_n} = \sqrt{\delta_n}$$

The eigenvalues, defined by (2.2) are numbered in order of increasing $|Y_n|$. For arbitrary α, spectral enumeration is in accordance with the order of the c_n for small α. The asymptotic expression for Y_n for large wave numbers can be written as

$$Y_n = -\alpha/R \qquad (n \ll \alpha) \qquad (2.3)$$

If $n \gg 1$, when R is bounded the eigenvalues are close to the corresponding values in a fluid at rest.

To determine the c_n in the interval between the asymptotic values, we use the numerical method of solving the eigenvalue problem for ordinary differential equations with a small parameter in the leading derivative developed in [4-6]. The numerical calculations were carried out on a BÉSM-6 computer. The eigenvalues were determined to a given accuracy (three significant figures). Control calculations were made for a Poiseuille flow and gave good agreement with the numerical results obtained in [7].

3. We trace the changes in the spectrum of small perturbations as A increases from zero for fixed $R = 10^5$. When $A = 0$ (Poiseuille flow), the numerical calculations give a spectral pattern which is completely analogous to that obtained in [6] for $R = 15{,}000$. Its characteristic feature is the precise separation of the perturbations, as the wave number increases, into two classes: boundary layer perturbations which are localized at the channel wall with phase velocity tending to zero, and internal perturbations which are localized on the channel axis with phase velocity tending to the maximum flow velocity.

The boundary layer perturbations are those with $n = 1, 2, 5, 8, \ldots$, while the internal perturbations are those with $n = 3, 4, 6, 7, \ldots$. When the plates move the typical feature of the subdivision of the perturbations is preserved in accordance with their behavior at large wave numbers. Among the boundary layer perturbations we distinguish upper and lower perturbations which are localized for large α at the upper and lower plates respectively.

Figures 1 and 2 show the behavior of $c_n(\alpha)$ for the first eight spectral numbers when $A = 0.15$. In this case the flow is unstable and the first eigenvalue leads to instability as in Poiseuille flow. Then the corresponding maximum of $Y_1(\alpha)$ is displaced in the direction of small α, and the instability is connected with the presence of a critical point on the lower plate. The critical point on the upper plate vanishes at much smaller values of A. The form of the subdivision of both the boundary layer and the internal perturbations remains of Poiseuille character through $n = 5$. However, perturbations corresponding to larger spectral numbers are distributed differently, viz., perturbations with numbers 6, 7 become lower boundary layer perturbations, while that with $n = 8$ becomes an internal perturbation.

In what follows we consider a finite number of spectral numbers beginning with $n = 1$, and so it is significant to note the preponderance of the number of lower boundary layer perturbations over upper pertur-

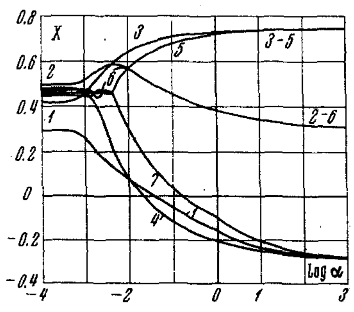

Fig. 3

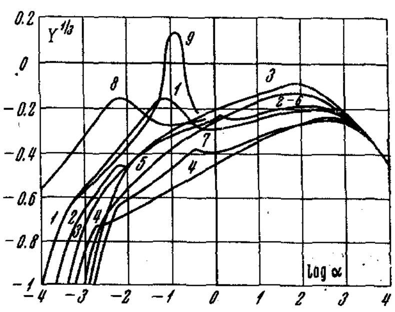

Fig. 4

bations and the general propenderance of boundary layer perturbations over internal perturbations, as distinct from the case of Poiseuille flow.

The behavior of X_n and Y_n as functions of α is given by the asymptotic expressions (2.1) and (2.2) for $\alpha \sim 10^{-4}$, and by the asymptotic expression (2.3) for $\alpha \sim 10^{4}$. Loss of stability of the velocity profile as A increases from zero leads to a change in the order in which the various eigenvalues belonging to different spectral numbers merge. If $c_3(\alpha)$, $c_4(\alpha)$ behave in the same way as in the Poiseuille case, i.e., they merge for small α, in other respects there are significant changes: the merging of boundary layer eigenvalues in the region $\alpha \gg 1$, which occurs for $A = 0$, is not observed. The corresponding functions $X_n(\alpha)$, $Y_n(\alpha)$ are markedly different from each other almost up to the asymptotic region. On the other hand, for small α the eigenvalues $c_5(\alpha)$ and $c_7(\alpha)$ merge. The complex intersection of $X_n(\alpha)$ and $Y_n(\alpha)$ and the local maxima of $Y_2(\alpha)$ and $Y_{5,7}(\alpha)$ for $\alpha \sim 1$, attract attention.

Near the maximum of $Y_{3,4}(\alpha)$ the corresponding eigenvalues separate at a low value and then later merge (this is not shown in Fig. 2).

Subsequent increase in A leads to a complex change in the spectrum. Figures 3 and 4 (curves 1-7) show $c_n(\alpha)$ for the first seven spectral numbers when $A = 0.3$. The perturbations are divided into boundary layer and internal perturbations as follows: numbers 1, 4, 7, ... correspond to lower boundary layer perturbations, numbers 2, 6, ... to upper boundary layer perturbations, numbers 3, 5, ... to internal perturbations. As A increases the separation of boundary layer perturbations into lower and upper is smoothed out. This is due to the reduction in the number of internal perturbations and due to changes in the distribution of the boundary layer perturbations. The eigenvalues $c_2(\alpha)$ and $c_6(\alpha)$ merge at approximately the same α as when $A = 0.15$.

The bifurcation of $Y_n(\alpha)$ becomes more marked when $\alpha \gg 1$, and this is clearly illustrated by $Y_1(\alpha)$ and $Y_{2,6}(\alpha)$. The most complex behavior of $c_n(\alpha)$ occurs for $\alpha = 10^{-3}$–10^{-2}, where the asymptotic expressions (2.1) and (2.2) essentially cannot be used. In the range of "dangerous" wave numbers there is a characteristic maximum of $Y_1(\alpha)$ and weaker maxima for $Y_{2,6}(\alpha)$ and $Y_7(\alpha)$.

When $A = {}^2/_3$ the velocity profile (1.3) loses its characteristic maximum inside the channel. Then the internal perturbations coincide with the upper boundary layer perturbations. Thus, for $A \geq {}^2/_3$ the spectrum of small perturbations only contains boundary layer perturbations. The preponderance of the number of lower boundary layer perturbations over upper boundary layer perturbations is also lost.

Figure 5 shows the behavior of $Y_n(\alpha)$ for the first four spectral numbers when $A = 0.75$. The separation of the boundary layer perturbation for this value of A into upper and lower occurs as follows: perturbations with $n = 1, 4, 5, 8, \ldots$ are lower boundary layer perturbations, those with $n = 2, 3, 6, 7, \ldots$ are upper boundary layer perturbations.

When α is in the range 10^{-4}–10^{-2} the functions $X_n(\alpha)$ and $Y_n(\alpha)$ intersect, but the various eigenvalues do not merge. (When $\alpha = 10^{-2}$ the eigenvalues are in the order of increasing $|Y_n|$ as follows: 1, 3, 2, 7, 5, 6, 4, 8, ... but as α changes this order is destroyed.)

In the above interval $Y_1(\alpha)$ has a weak local maximum.

Similar maxima are traced in Figs. 2 and 4, but in these cases they are forerunners of the merging of the various eigenvalues at the points of discontinuity of $c_n(\alpha)$. The Y_n no longer have local maxima in

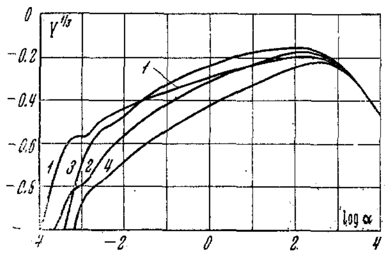

Fig. 5

the region of dangerous α. In this case their behavior recalls that of the internal perturbations in the cases discussed. We note that, as distinct from Couette flow (cf [8]), the first eigenvalue is not everywhere the most dangerous here.

To trace the nature of the transition to Couette flow numerical computations were made for values of A close to unity. The various $c_n(\alpha)$ have typical Couette discontinuities for small α beyond the asymptotic region, which are connected with the occurrence of oscillatory perturbations when A = 1. In the Y plane the separate eigenvalues corresponding to the upper and lower boundary layer perturbations, which merge for A = 1, approach each other. The spectrum of small perturbations of Covette flow has been studied by a number of authors. The case of large Reynolds numbers was studied in detail in [8].

4. We consider the behavior of the perturbations as a function of the Reynolds number. It is easy to see that Eq. (1.1) is approximated well by the following equation when $\alpha^2 \ll 1$:

$$\varphi^{IV} = i\alpha R\,[(u-c)\,\varphi^{II} - u''\varphi] \qquad (|c \pm A| \gg \alpha^2) \tag{4.1}$$

From this equation we see that the eigenvalues depend only on one parameter αR. Thus, knowing the numerical results for one R we can a priori draw conclusions about the behavior of $c_n(\alpha)$ for other values of R when $\alpha^2 \ll 1$ which is a wider region than that in which (2.1) and (2.2) are valid.

The range of α in which the above considerations hold is very interesting since a significant reorganization of the spectrum by comparison with the asymptotic behavior takes place.

This can be used in numerical calculations at various Reynolds numbers. As an example, Fig. 4 shows $Y_1(\alpha)$ for $R = 10^6$ (curve 8) and $Y_1(\alpha)$ for $R = 10^5$, which illustrate the validity of the approximation of the Orr-Sommerfeld equation by (4.1) when $\alpha^2 \ll 1$.

In the previous section we drew attention to the existence of local maxima for some of the $Y_n(\alpha)$. The greatest interest lies in the behavior of these maxima as R increases since their existence can be linked to an additional instability. Numerical calculations in which both "continuous motion" [4] and the approximation considered here are studied show that the instability of the Couette-Poiseuille flow is only connected with the first eigenvalue.

The value of A which completely stabilizes the flow was found using continuous motion from the maximum of $Y_1(\alpha)$. It was A = 0.26, which corresponds to the results of [1, 2]. Fig. 4 (curve 9) shows $Y_1(\alpha)$ for A = 0.23, $R = 10^5$. For these parameters the flow is not yet unstable.

The author wishes to thank M. A. Gol'dshtik for his attention to the paper, V. A. Sapozhnikov for useful discussions, and V. N. Shtern for his great assistance and help with the paper and for useful discussions.

LITERATURE CITED

1. M. C. Potter, "Stability of plane Couette-Poiseuille flow," J. Fluid Mech., 24, pt. 3 (1966).
2. F. D. Hains, "Stability of plane Couette-Poiseuille flow," Phys. Fluids, 10, No. 9 (1967).
3. R. V. Birikh, G. Z. Gershuni, and E. M. Zhukhovitskii, "The spectrum of perturbations of plane-parallel flows at small Reynolds numbers," Prikl. Matem. i Mekhan., 29, No. 1 (1965).
4. M. A. Gol'dshtik and V. A. Sapozhnikov, "The stability of laminar flow when there is a body force field," Izv. Akad. Nauk SSSR, Mekhan. Zhidk. i Gaza, No. 5 (1968).
5. V. A. Sapozhnikov, "Solution of the eigenvalue problem for ordinary differential equations by the pivotal condensation method," in: Proceedings of the All-Union Seminar on Numerical Methods in the Mechanics of Viscous Fluids (II) [in Russian], Nauka, Novosibirsk (1969).
6. V. A. Sapozhnikov, M. A. Gol'dshtik, and V. N. Shtern, "Local properties of the velocity profile and hydrodynamical stability," 2nd Republican Conference on Heat and Mass Transfer (Abstracts of Proceedings), Kiev, 1969.
7. V. A. Sapozhnikov and V. N. Shtern, "The numerical analysis of the stability of plane Poiseuille flow", Zh. Prikl. Mekhan. i Tekh. Fiz., No. 4 (1969).
8. V. N. Shtern, "The spectrum of small perturbations of plane Couette flow," Zh. Prikl. Mekhan. i Tekh. Fiz., No. 1 (1970).